Master's Thesis of Jongmin Rim

Advanced Permeability Analysis of Smart Structural Composites using Gray Lattice Boltzmann Method

회색 격자 볼츠만 방법을 이용한 스마트 구조 복합체의 고급 투수 해석

February 2023

Graduate School of Engineering
Seoul National University
Civil & Environmental Engineering Major

Jongmin Rim

Advanced Permeability Analysis of Smart Structural Composites using Gray Lattice Boltzmann Method

Jae-Yeol Cho

Submitting a master's thesis of
Civil & Environmental Engineering

February 2023

Graduate School of Engineering
Seoul National University
Civil & Environmental Engineering Major

Jongmin Rim

Confirming the master's thesis written by
Jongmin Rim
February 2023

Chair	____________________	(Seal)
Vice Chair	____________________	(Seal)
Examiner	____________________	(Seal)

Abstract

Smart maintenance of built environments is gaining more importance due to the aging of the structures. Since the built environments are mostly constructed with concrete, durability assessment methods such as permeability analysis and ionic diffusivity analysis have been utilized. Meanwhile, accurate simulation method for predicting the durability performance has not been well developed due to the complexity of materials. Experimental methods need large sample from built structure and long time, and numerical methods have limitations due to the resolution of the pore structures and complex boundaries.

In this study, the permeability analysis is performed with the lattice Boltzmann method to overcome those limitations. The focus of the study is on development of efficient image-based lattice Boltzmann method that considers effect of pore structures below image resolution. The gray lattice Boltzmann method (GLBM) with hybrid MPI-OpenMP parallelization is proposed and implemented. The stability and accuracy of the code are tested for mortar samples with interconnected pore structures. The gray lattice Boltzmann simulation is conducted for the cement samples with different water to cement ratio which have percolated pore structures in images due to the resolution. The results show high accuracy with improved time of simulation. The method developed herein can be utilized for smart maintenance of infrastructure. Furthermore, overcoming limitations in image-based numerical methods for porous composites is suggested as a future study.

Keyword：The Lattice Boltzmann Method, Computed Tomography

Student Number：2021-20709

Table of Contents

Chapter 1. Introduction

1.1. Study Background

Concrete and cementitious materials are the most used materials for the construction of the buildings and infrastructures next to water. The ages of the structures around world are growing and the cost for the maintenance of the structures are increasing conforming to this trend. Therefore, assessment for durability of the built structures is gaining more importance to increase the efficiency of the maintenance and safety of the structures. The durability of the concrete structures is highly influenced by the water and ion transportation inside the concrete materials. The transportation phenomena inside the material affect the mechanical properties of the structure itself and also result in deterioration of the steels in concrete. These phenomena happen dominantly by water transportation as the ions moves inside the material as dissolved form in water. As a result, durability assessment is conducted by assessing the transportation of water and ions. There are several codes for the assessment of these transportation such as water absorption test (ASTM C1585 [1]), cyclic freeze-thaw tests (ASTM C666 [2]), chloride diffusivity test (ASTM C1556 [3]). These methods are mostly based on lab test with samples composed of same materials as built structure or comparably large samples obtained from the site. However, there are unavoidable gap between lab test and built structure as the test takes large time for the experiment to reach stationary state. This large time for the experiment and difficulty in acquisition of the samples leads to the inaccurate and inefficient assessment. Therefore, numerical methods using 3D X-ray micro computed tomography have been developed.

Numerical methods to determine the water permeability have been proposed with various schemes such as Finite Volume (FV) [4] and Finite Element (FE) [5] method employing Navier Stokes Equation (NSE) for the analysis. However, these methods encounter complexity of the porous geometry and boundary condition problems. Also, probabilistic methods using 3D X-ray micro computed tomography such as Monte Carlo simulation and random walker simulation [6] have been developed and tested for water permeability. Even if probabilistic methods can overcome problems due to the complexity of geometry and boundary conditions, these methods have weak relations between physical properties and simulation parameters which raises questions about the solid relationship between physical phenomena.

Beside the problems aforementioned, these computational methods consume large computational resources and time, and also are highly dependent on the resolution of the micro computed tomography. The numerical methods additionally exhibit instability when dealing with complex geometry. As solution for the NSE gives fluid flow in void, the resolution determines the flow system in the media and therefore, insufficient resolution would give significant difference between experiment and the numerical simulations. The effect of the void smaller than resolution such as capillary pores should be incorporated to reconstruct real fluid system inside the concrete materials. This effect can be resolved by solving Stokes-Brinkman equation instead of NSE. Stokes-Brinkman equation solves NSE for void and implement Darcy's 2^{nd} law for permeable media.

1.2. Purpose of Research

Concrete has complex micro to macro scale pore structures that is not available for complete acquisition. Also, high mesh density for the numerical methods consumes high computational costs and time which would diminish the advantages of the methods. Therefore, this study intends to reduce mesh density of the numerical simulation and increase efficiency of the simulation by high performance computation. In addition, simulation aims to utilize capillary pore effect for concrete and cementitious materials. In this study, the gray lattice Boltzmann method is implemented for concrete to solve Stokes-Brinkman equation. In-house code for the lattice Boltzmann method is tested for the connected pore systems obtained from cemented sandstone samples to validate the methods.

The gray lattice Boltzmann method is adopted for the ordinary Portland cement (OPC) samples with different water-to-cement ratios. 3D micro computed tomography images are converted to binary images of pore structure, hydrated materials and anhydrous materials. As the hydration occurs at the interface of water and clinkers, hydrated materials (C-S-H, CH, Afm and Calcite) are assumed as permeable media and anhydrous materials (C_3S, C_2S, C_4AF) are assumed as impermeable media. Permeability characteristics of the hydrated materials are estimated by comparing porosity of the samples obtained from micro computed tomography and that obtained from hydration degree and Powers equation. The hydration degrees of the samples are estimated by thermogravimetric analysis (TGA) results. The simulation is carried out with in-house code with MPI-OpenMP hybrid parallelization and results are compared with literatures and previous researches.

Chapter 2. Methodology

2.1. Sample Preparation for Cemented Sandstone

Different samples for the validation and simulation of the lattice Boltzmann method and the gray lattice Boltzmann method are made. The mortar specimen [6] is used for the validation of the lattice Boltzmann method which is the method for the interconnected pore structures. The mortar specimen is composed of Jumunjin sand and ordinary Portland Cement (OPC) with tap water. Samples are prepared with different sand-to-cement ratio of 0, 1, 3, 5 and 7%. The water contents of the samples are fixed. The samples are cast in polyvinyl chloride (PVC) molds with a diameter of 2.5cm and a height of 2.5 cm and are cured at 20°C for 7 days. X-ray tomographic images are acquired with X-ray scanner (Skyscan1272, Bruker, Belgium) with pixel resolution of 5μm. These images are processed with Gaussian blur and anisotropic diffusion filter and then converted into binary images with Otsu's method as described in Pae's research [6]. But binary images are not processed with watershed algorithm as the previous research.

2.2. Sample Preparation for Ordinary Portland Cement

Ordinary Portland cement samples with different water-to-cement ratio of 0.3, 0.4, 0.5, 0.6 and 0.7 are used for the gray lattice Boltzmann method. The samples are cast in straw with a diameter of 3mm and cured at 20℃ with relative humidity of 60% for 28 days. X-ray tomographic images are acquired with same X-ray scanner as the mortar samples with pixel resolution of 0.5μm as depicted in Fig 1. The VOI (Volume of Interest) is cropped with size of $1.5\times1.5\times1\ mm^3$ as given in Fig 2.

Figure 1. Specimen in straw

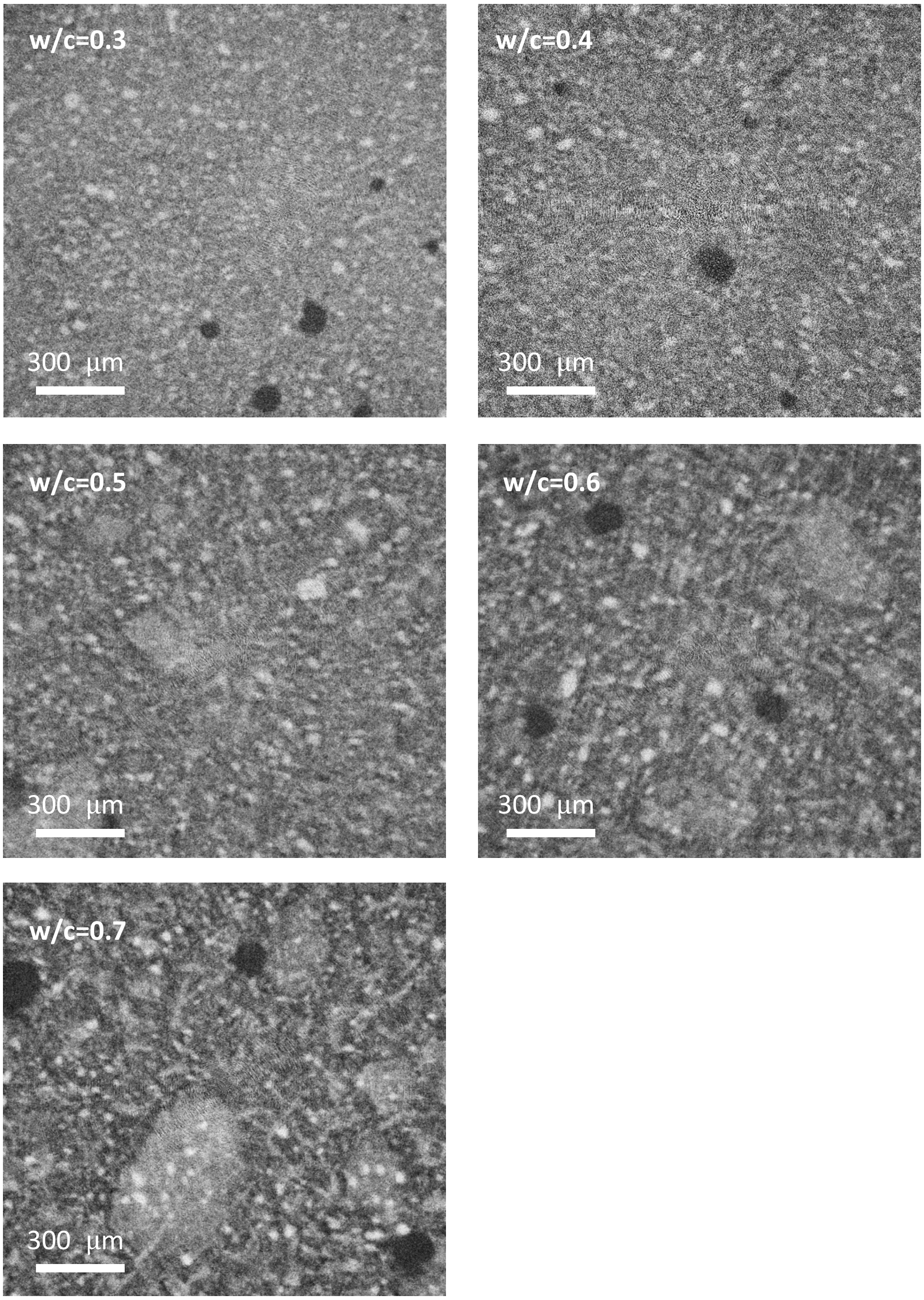

Figure 2. 3D micro computed tomography of OPC samples

Different materials pose different linear attenuation coefficient (LAC) of X-ray. The LACs of pore, hydrated and anhydrous phases can be calculated by the LAC's weighted averages of the materials for each phase. The weight of each material can be determined by the mass fractions which is calculated by QXRD data in Fig 3. The LACs of each phase are described in Fig 4. The threshold values for each phase are calculated with the intersection point of Gaussian distribution of grayscale values of the pixels obtained by LACs for each phase as described in Fig 5. The binary images of pores, hydrated and anhydrous phases are obtained from these threshold values and 3D structure of the OPC samples were reconstructed as Fig 6.

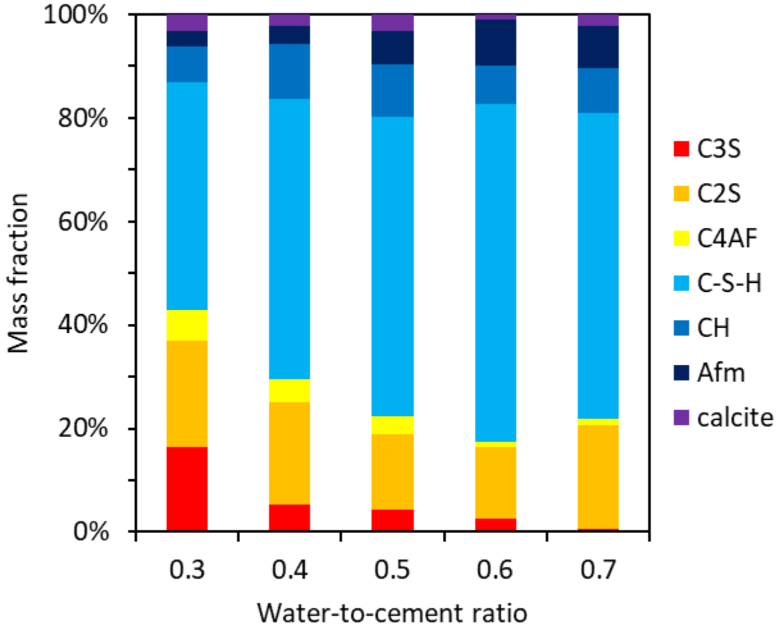

Figure 3. Mass fraction of the materials

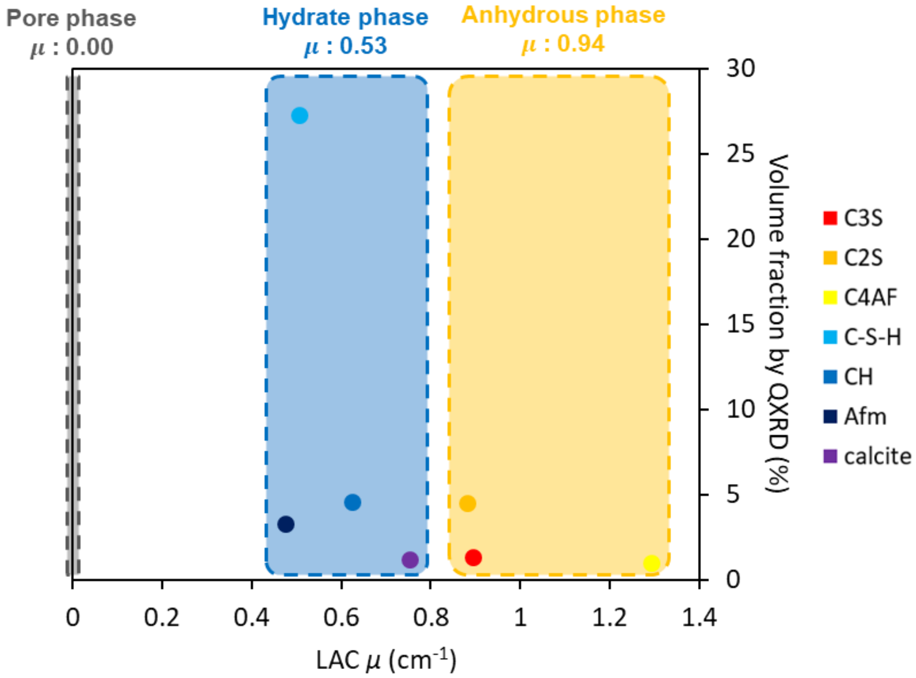

Figure 4. LACs of each phase

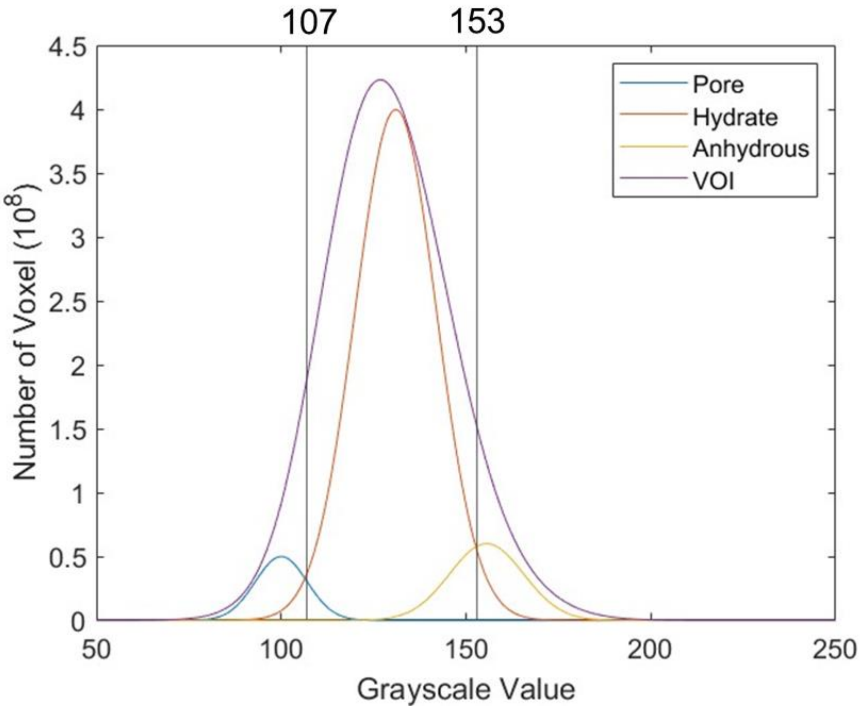

Figure 5. The threshold values for each phase

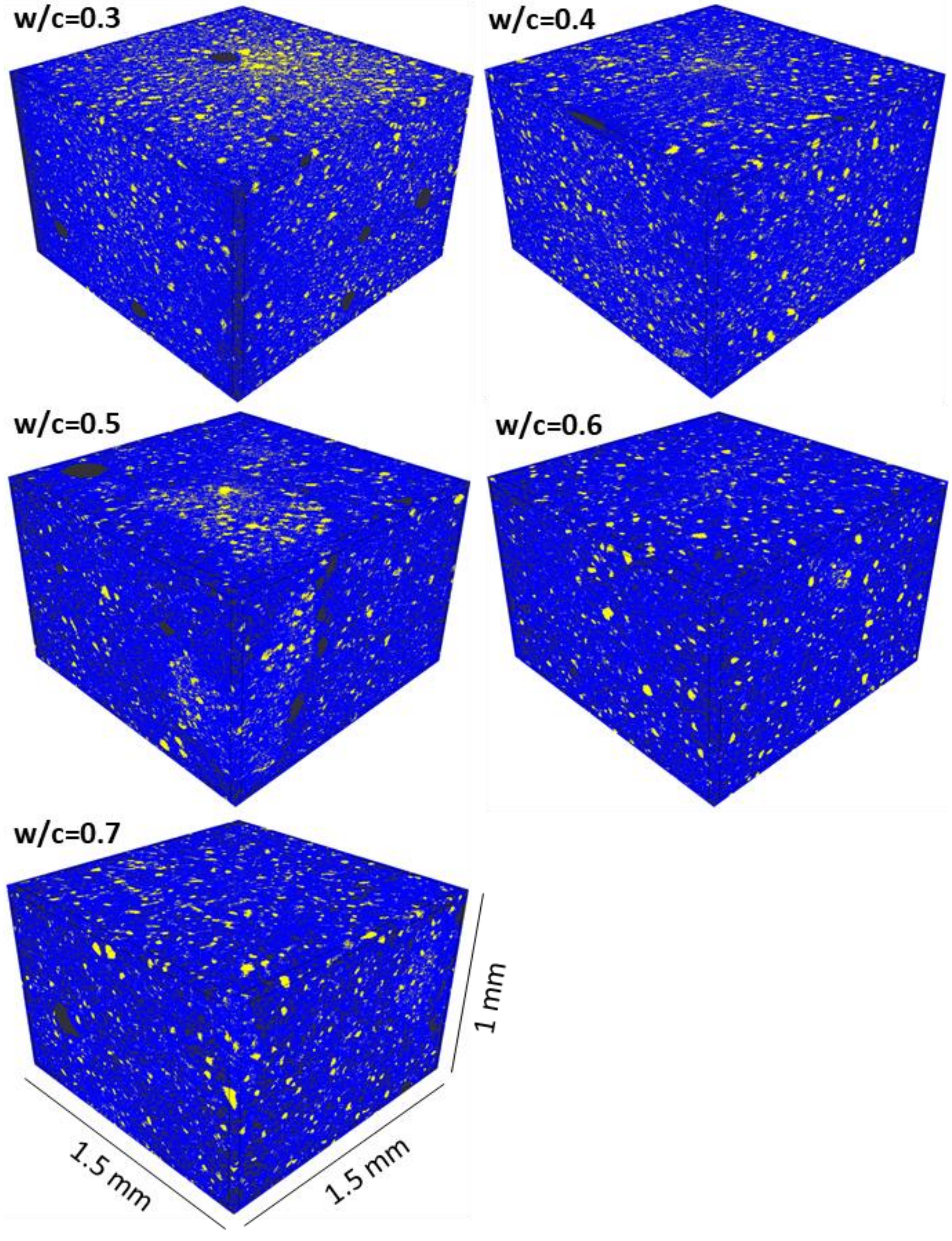

Figure 6. 3D reconstruction of OPC samples

2.3. The Lattice Boltzmann Method

Boltzmann equation is the partial differential equation which describes the probability of the particles at certain position and time with specific velocity. The equation is written as follows.

$$\frac{\partial f(\mathbf{x},\ \mathbf{v},\ t)}{\partial t} + \mathbf{v} \cdot \frac{\partial f(\mathbf{x},\ \mathbf{v},\ t)}{\partial \mathbf{x}} + \frac{\mathbf{F}}{m} \cdot \frac{\partial f(\mathbf{x},\ \mathbf{v},\ t)}{\partial \mathbf{v}} = \Omega(f). \tag{1}$$

where $f,\ \boldsymbol{x},\ t,\ \boldsymbol{v}, \boldsymbol{F}, m, \Omega$ each denotes density function, position, time, velocity, force, density of fluid in physical unit and collision operator, respectively. Collision operator determines the evolution of the particle probability function. Therefore, collision operator should obey the physical principles such as mass and moment conservation and equation of state.

As the equation describes general particle behavior, the LGA (Lattice Gas Automata) was proposed for gas flow. Discretization of dimensionless form of Boltzmann equation in space, time and velocity using Hermite polynomial and Chapman-Enskog expansion gives the discretized form of Boltzmann equation for each discretized velocity which enables to obtain numerical solution of the gas flow. LGA was extended to the general fluid cases that are described by NSE (Navier-Stokes Equation). Discretized Boltzmann equation can be written as follows.

$$f_i^{out}(\mathbf{x} + \mathbf{e}_i \Delta t,\ t + \Delta t) = f_i^{in}(\mathbf{x},\ t) + \Delta t \Omega_i\left(f_i^{in}\right) \tag{2}$$

where $f_i, \boldsymbol{x}, t, \boldsymbol{e}_i, \Omega_i, \Delta t$ denoting density function discretized in velocity sets, position, time, discretized velocity, collision operator discretized in velocity sets and time step in lattice unit. The discretization using Chapman-Ensokog expansion which is the kind of perturbation expansion with Knudsen number guarantees second order accuracy in time, space and velocity for no-boundary case flows. Collision operator for each velocity can be selected with condition that the operator preserves mass and momentum. In most cases where viscosity difference and turbulence are not large, SRT (single relaxation time) model can be implemented which usually employs BGK operator. However, SRT model use only one relaxation time that relates the parameter (relaxation time) which controls stability of the simulation to physical property i.e., viscosity. This property of SRT model leads to the divergence of the simulation and stability problem for some cases. If the SRT model can't give stability and accuracy, TRT (Two relaxation time) or MRT (Multi relaxation time) model should be implemented. They employ additional relaxation time that relaxes the moment of different order with different ratio which remedies the problem of relating stability and physical property. In this study, SRT model is sufficient for the simulation and therefore BGK operator is employed which can be given as follows. [7]

$$\Omega_i(f_i) = -\frac{1}{\tau}\left(f_i^{in} - f_i^{eq}\right) \tag{3}$$

$$\left(\text{where } f_i^{eq} = w_i\rho\left[1 + \frac{\boldsymbol{e_i}\cdot\boldsymbol{u}}{c_s^2} + \frac{(\boldsymbol{e_i}\cdot\boldsymbol{u})^2}{2c_s^4} - \frac{\boldsymbol{u}\cdot\boldsymbol{u}}{2c_s^2}\right],\ c_s^2 = \frac{1}{3}\left(\frac{\Delta x}{\Delta t}\right)^2\right)$$

where $f_i^{eq}, w_i, \rho,\ \Delta x, \tau$ each denotes equilibrium distribution which is derived from discretization of Boltzmann distribution, weight for each discretized velocity, density in lattice unit, size of lattice in lattice unit and relaxation time of simulation.

The population function and macroscopic variables such as density, velocity and energy are related as follows.

$$\rho = \sum_{i=0}^{18} f_i \ , \mathbf{u} = \frac{1}{\rho}\sum_{i=0}^{18} f_i \mathbf{e}_i \ , E = \frac{1}{\rho}\sum_{i=0}^{18} f_i \, |\boldsymbol{e}_i|^2 \tag{4}$$

$$(\mathrm{E} = \text{energy of the unit lattice})$$

Substituting equation (3) into (2) and separating equation (2) into two steps with individual lattice operation and inter-lattice operation gives equation (5) and (6).

$$f_i^*(x,t) - f_i^{in}(x,t) = -\frac{1}{\tau}\left(f_i^{in}(x,t) - f_i^{eq}(x,t)\right) \tag{5}$$

$$f_i^{out}(x + e_i \Delta t, t + \Delta t) = f_i^*(x,t) \tag{6}$$

Equation (5) describes collision step of particles in unit lattice and physical meaning of relaxation time can be understood as time distance between particle collision which is parameter for the simulation. The population function with asterisk indicates the function after the collision. Equation (6) describes streaming step after collision, this separation makes LB for easy parallelization as collision process of lattice cells are independent of other adjacent cells and complex boundary conditions and molecular interactions can be adopted with modified collision terms and equilibrium function.

In this study, D3Q19 model which means unit cell with 3 dimensions and 19 velocities set is implemented for both LB test cases and GLB cases to assure stability and accuracy of the simulation [7].

For permeability analysis of the domain, periodic constant pressure boundary condition is imposed and periodic boundary condition is imposed for 4 surface planes of the domain. The no-slip boundary condition was imposed for the solid-fluid interface. Equivalent boundary condition for no-slip boundary condition in the lattice Boltzmann method is called bound-back boundary condition which is described as follows.

$$f_i^{out}(\boldsymbol{x} + \boldsymbol{e}_i \Delta t, t + \Delta t) = f_{\bar{i}}^{*}(\boldsymbol{x}, t) \tag{9}$$

Since $\bar{\imath}$ is the velocity component opposite to i, bounce-back boundary condition implies that the particles bounce back to the opposite direction when it collides with rigid wall. In this study link-wise half-way bounce-back boundary conditions are imposed for solid-fluid interface.

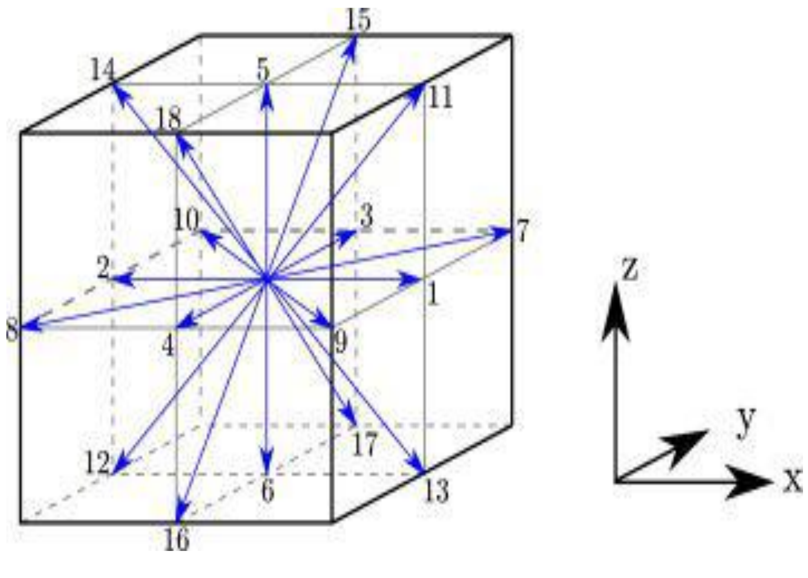

Figure 7. D3Q19 model

2.4. The Gray Lattice Boltzmann Method

In this study, following Stokes-Brinkman equation is introduced to describe the isothermal incompressible fluid system with pores, permeable media and impermeable media.

$$\nabla \vec{u} = 0 \tag{7}$$

$$\nu K^{-1}\vec{u} + \frac{1}{\rho_0}\nabla \vec{P} - \vec{g} = \frac{\nu_e}{\phi}\Delta \vec{u} \tag{8}$$

For the Stokes flow in pore structure, above equation recovers Stokes equation, where $\vec{u}$, ν, K, $\rho_0, P, g, \phi, \nu_e$ each denotes velocity vector, kinematic viscosity, permeability tensor, reference density, pressure, gravity acceleration, porosity and effective viscosity.

In the kinematic point of view, Dardis and McCloskey [8] proposed partial bounce-back boundary condition for flow through permeable media which is modification of the bounce-back method. And Walsh et al [9] examined the previous partial bounce-back schemes and proposed new partial bounce-back boundary condition that conserves mass and recovers the finite difference formulation of Stokes-Brinkman equation. In this study, partial bounce-back boundary condition proposed by Walsh (Walsh PBB) is utilized for Darcy flow region which reads.

$$f_i^{out}(\boldsymbol{x} + \boldsymbol{e}_i\Delta t, t + \Delta t) = (1 - n_s)f_i^{*}(\boldsymbol{x}, t) + n_s f_{\bar{i}}^{in}(\boldsymbol{x}, t) \tag{10}$$

where n_s is solid fraction of the cell. The physical meaning of the partial bounce-back is that the constant ratio of the particles after collision pass through the cell and rest of the particles came in from opposite direction are bounced back. Therefore, solid fraction value of 0 recovers free-flow channel while value of 1 doesn't exactly recovers fluid-solid interface with bounce-back boundary conditions as the collision step is not conducted for the case. Therefore, the bounce-back boundary condition is adopted for impermeable media which is anhydrous phase and Walsh partial bounce-back boundary is adopted only for permeable media which is hydrated phase. The simulations for the gray lattice Boltzmann method also used same domain boundary conditions as the cemented sandstone cases other than partial bounce-back boundary.

The size effect of the unit cell for the LBM simulations which is reported by Succi [10]. A channel with a unit cell width magnifies the flow velocity which results in exaggerated permeability value. Therefore, the lattice resolutions are increased for OPC samples. However, increase in the lattice resolution results in augmented consumption of the computational resources, especially memories. Therefore, the increase in the lattice resolution results in smaller domain which raises problem for the representativeness of the volume used for the simulation. This problem is more important for high water-to-cement ratio samples which poses more heterogeneous pore structures than samples with low water-to-cement ratio. In this study, the lattice resolution for the water-to-cement ratio of 0.3 and 0.4 is increased to 4 times and otherwise to 2 times to balance the size effect and assure representativeness of the simulations.

2.5. The Solid Fractions of Hydrated Phase

The solid fraction of permeable media is proportional to capillary porosity inside the hydrated phase. Therefore, total porosity and the porosity obtained from the binary images are compared to obtain the solid fraction of permeable media. Powers equation gives the estimation of the total porosity in cement composites from w/c ratio and hydration degree with following form.

$$V_p = \left(\frac{w}{c} - 0.36H\right) \times \left(\frac{w}{c} + 0.32\right) \quad (11)$$

Hydration degrees of each sample are obtained from the thermogravimetric analysis data in Fig 8 and volume fractions of each phase are obtained. The results are depicted in Fig 9.

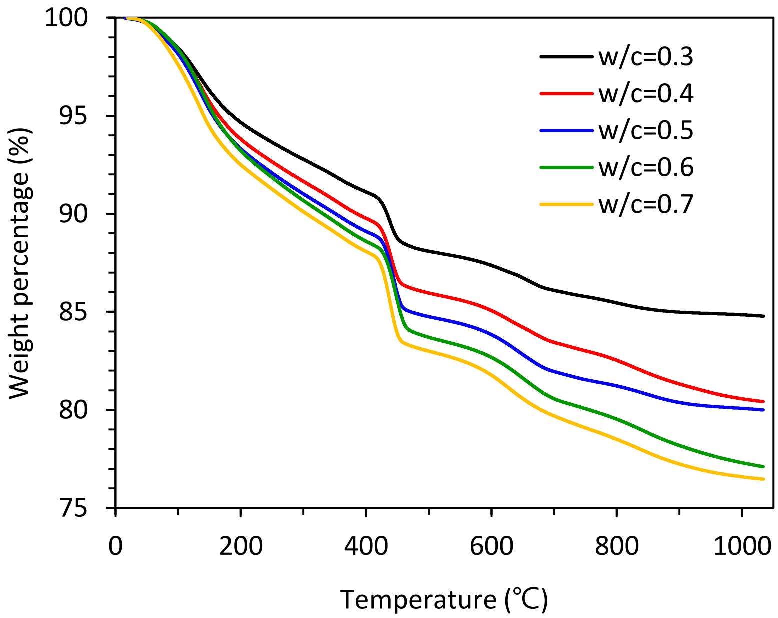

Figure 8. Thermogravimetric analysis of OPC samples

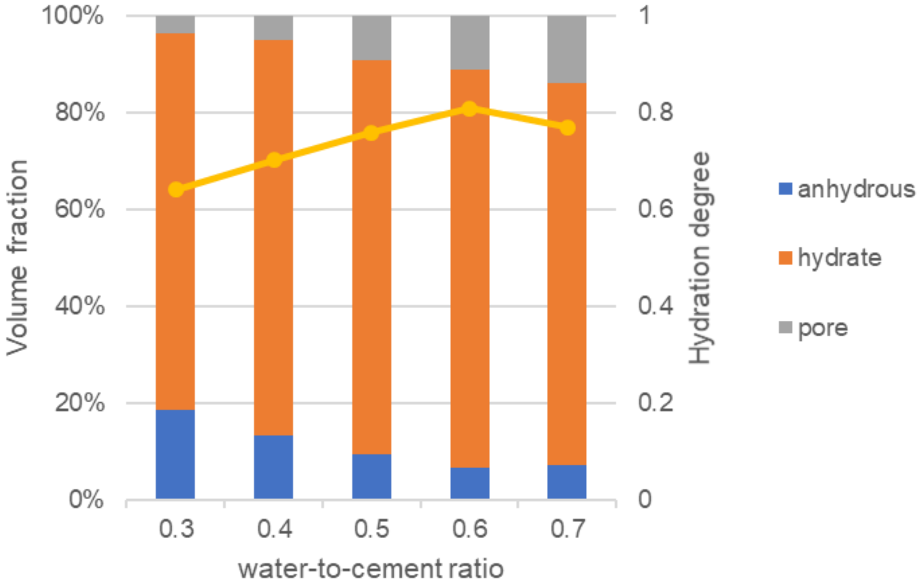

Figure 9. Volume fractions of each phase and hydration degrees of OPC samples

Therefore, unresolved volume fraction of porosity in hydrated phases can be calculated from total porosity of Powers equation, resolved porosity from micro computed tomography and volume of hydrates. Solid fraction of the hydrated phases can be calculated by substituting porosity from 1 and the results are illustrated in Table 1.

W/C ratio	0.3	0.4	0.5	0.6	0.7
Porosity (CT) (%)	2.97	6.29	9.28	10.98	13.83
Porosity (Power) (%)	11.17	20.42	27.65	33.58	41.43
Solid Fraction	0.883	0.844	0.781	0.683	0.573

Table 1. Solid Fraction of Specimen

2.6. Hybrid MPI-OpenMP Parallelization

In the purpose of utilizing exceptional capability of the lattice Boltzmann method for the parallelization, hybrid MPI-OpenMP parallelization is adopted for the simulation. The domain is divided into subdomains containing equal number of cells. If the total number of cells is divisible with number of processors, the quotient multiplied by the number of cells on the same plane is divided into each processor then the remainder multiplied by the number of cells on the same plane is added to the processor with smaller rank sequentially until the cells are all distributed. Each processor has its buffer memory with size of plane multiplied by number of processors it should communicate for MPI communication of population function with processor containing adjacent cells. The schematic diagram of the scattering of the domain is depicted in Fig 10.

For each processor, OpenMP loops with scheduled clauses are utilized to process collision operation and stream inside the subdomain. Then total energy of the subdomain is derived with reduction clauses. Then MPI communication is utilized to stream using non-blocking communication and calculated total energy of total domain using reduction clauses. The flowchart of the process is depicted in Figure 11.

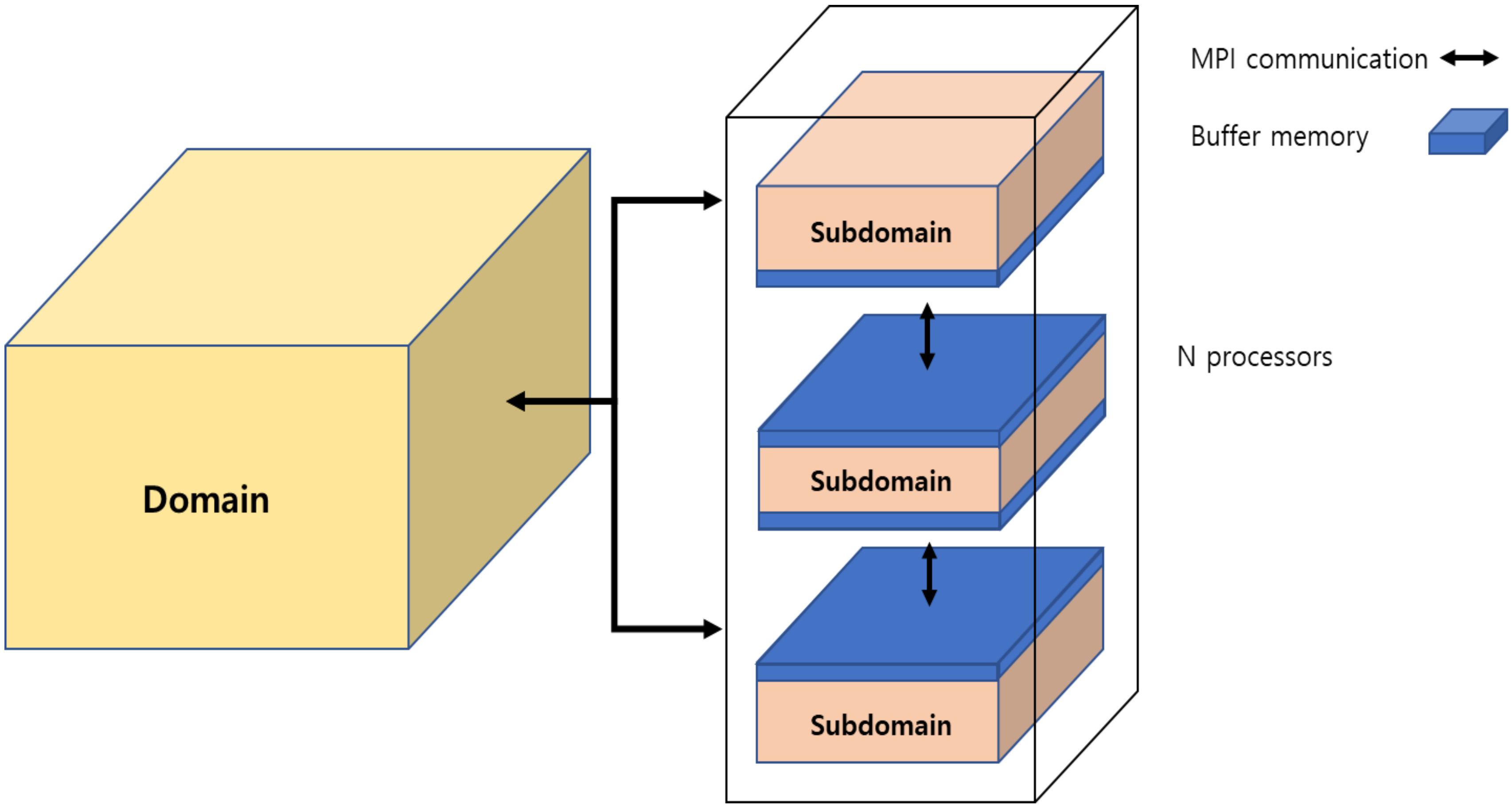

Figure 10. Schematic diagram of the parallelization

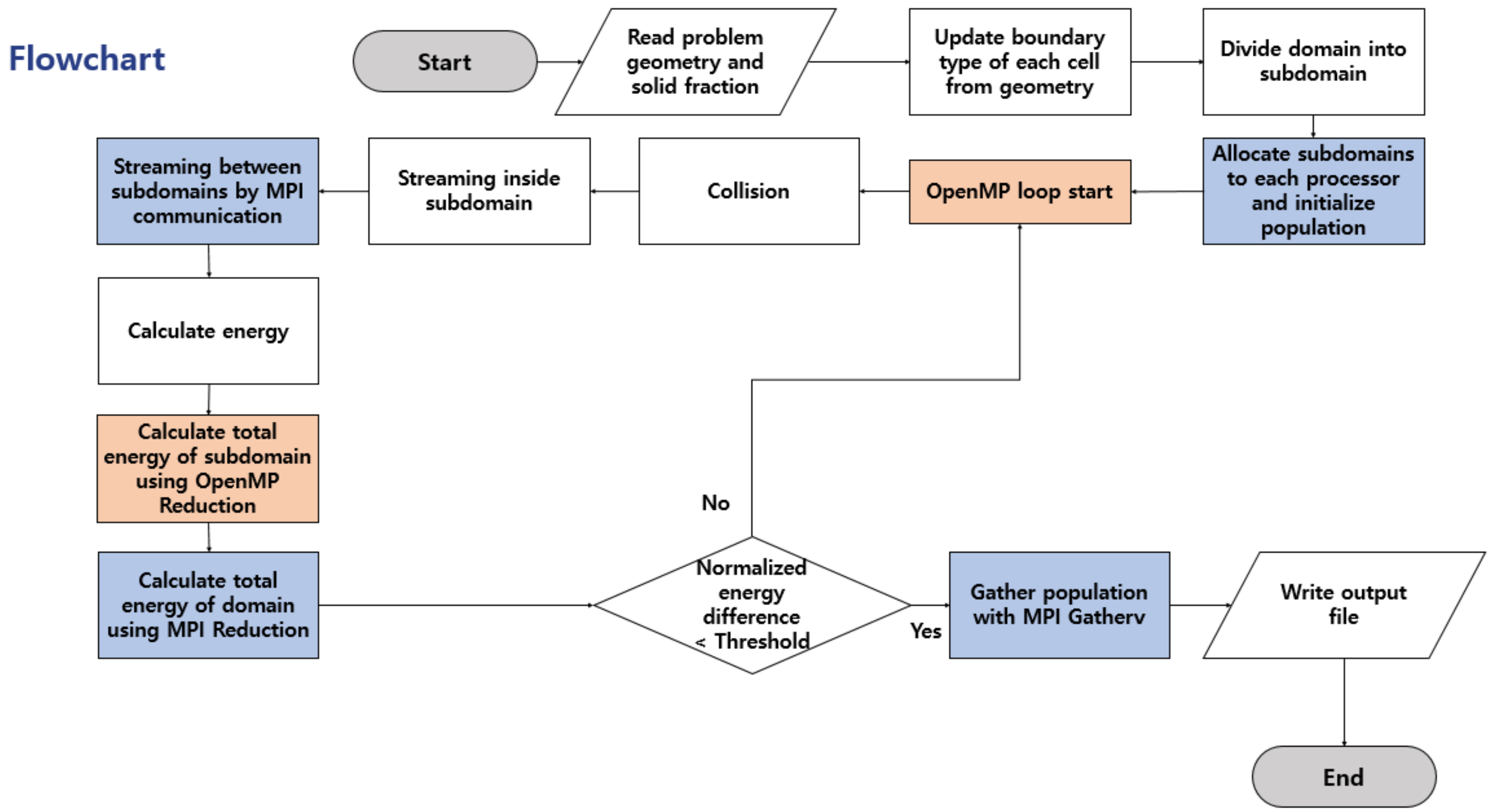

Figure 11. Flowchart for parallelization strategy

Chapter 3. Results and Discussion

3.1. The Lattice Boltzmann Method

The lattice Boltzmann method showed considerably accurate result compared to random walker simulation which showed good agreement with experimental data. Error of simulation which was calculated with energy difference between previous and present iteration showed monotone decreasing function guaranteeing stability of the simulation and converged with threshold value of 10^{-6}.

S/C ratio	0.0	0.1	0.3	0.5	0.7
Random walker (μm^2)	168.75	271.14	142.35	109.23	79.53
LBM (μm^2)	168.5	267.5	189	123.25	103.75

Table 2. Absolute permeability of cemented sandstone sample.

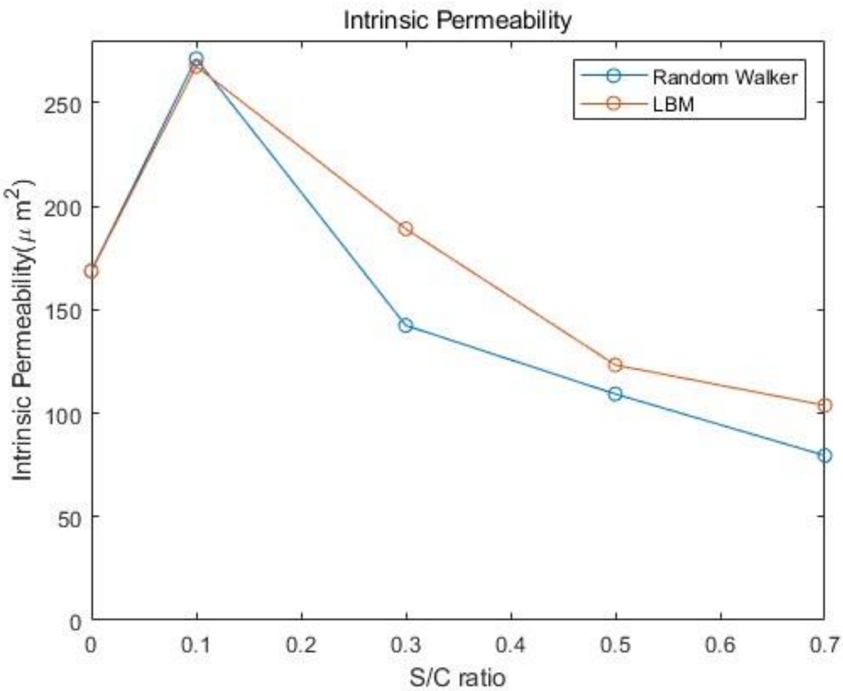

Figure 12. Intrinsic water permeability of cemented sandstone to sand to cement ratio.

The results show great compatibility but value slightly varies at 0.3, 0.5 and 0.7. The reason of the different values is due to the image processing qualities, as the random walker and the lattice Boltzmann simulation are conducted with binary images with different qualities as proposed in the Figure 13.

The test case for cemented sandstone showed the accurate and efficient simulation capability of the lattice Boltzmann method and the importance of image processing procedures.

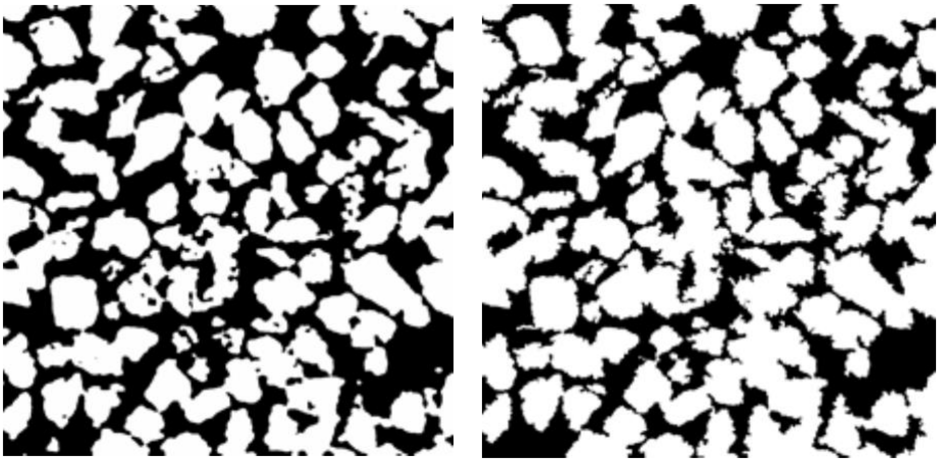

Figure 13. Same image with different quality

3.2. The Gray Lattice Boltzmann Method

The gray lattice Boltzmann method could simulate the transport of water through disconnected pore with comparably high speed due to the hybrid parallelization. Additionally, similar tendency of permeability is achieved compared to the experimental data in literature [11] as given in Fig 14. The intrinsic permeability increased as even degree function as the water-to cement ratio increased. However, the absolute values have different scales compared to intrinsic permeability of the concrete obtained from the experiments. This phenomenon has been reported in other researches [12] [13] related to simulation of permeability in cementitious materials while the scale of the permeability characteristics at low degree of water saturation was well captured. The gap between the experiment and simulation can be explained with following reasons. First, the simulation assumes the full saturation of the pore structures which is the ideal state of the experiment. Even if the experiment consumes long time to reach stationary state, full saturation of the pore structure is not available. In addition, the hydration during the experiment results in the difference. As the time duration for the experiment is at least a week, the hydration process would change the pore structures. If the stationary state is attained, the permeability calculated is not that of the samples at 28 days resulting in lower intrinsic permeability.

In addition, the results are compared to the porosity and permeability relationship derived by the lattice Boltzmann simulation with hydration model in literature [14]. The gray lattice Boltzmann simulation showed great agreement of the values from the literature. Fig 15 shows the GLBM results and the values from the literature. The GLBM results are plotted with porosity obtained by Powers equation. Therefore, the solid fractions used for the

GLBM recovered the permeability characteristics of the permeable media i.e., hydrated materials. Also, the samples with water-to-cement ratio of 0.3 and 0.4 that are not able to be simulated with the lattice Boltzmann method could be simulated with the GLBM and gave comparably accurate results.

Furthermore, the visualization of the GLBM results in Fig 15 shows the flow path through pore and hydrated phases. It proposes the importance of the capillary pore effects in the transport characteristics of cementitious materials as a numerical method. Previous simulations carried out is not available to consider capillary pore effects as the transport was impossible for actual samples while the permeability values have been measured with experiments.

Nevertheless, there are several further improvements demanded for the method.

1. As the durability analysis method, the observations about saturation effect address the need for the simulations with the boundary conditions that represent the actual environment where the structure is built.
2. For the two phases flow with gas and water which determines the degree of saturation, absorption and release of gas and water under the resolution should be dealt with the methods like GLB to investigate the saturation effect for the systems with disconnected pores.
3. In this study, permeability characteristics have been determined by rough approximation with porosity, however, to improve the method for tomography-based durability analysis, further understanding of capillary pore systems should be investigated.

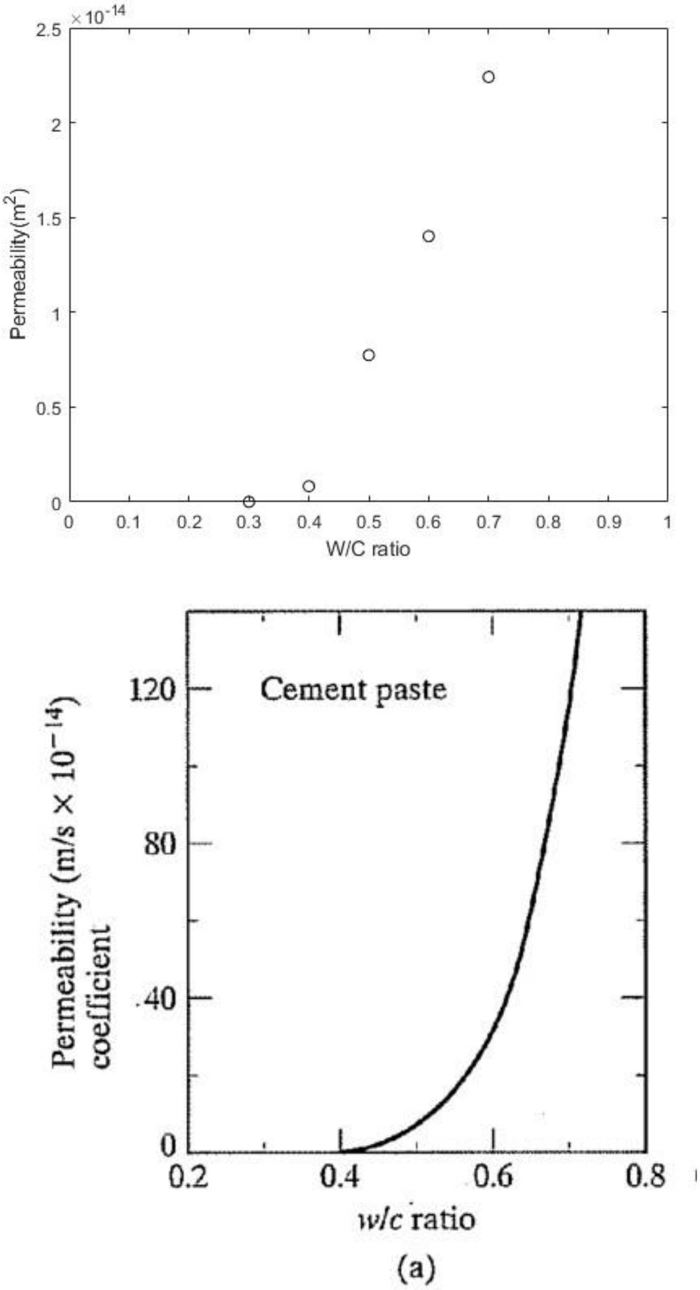

Figure 14. Intrinsic permeability to W/C ratio graph of simulation and experiment

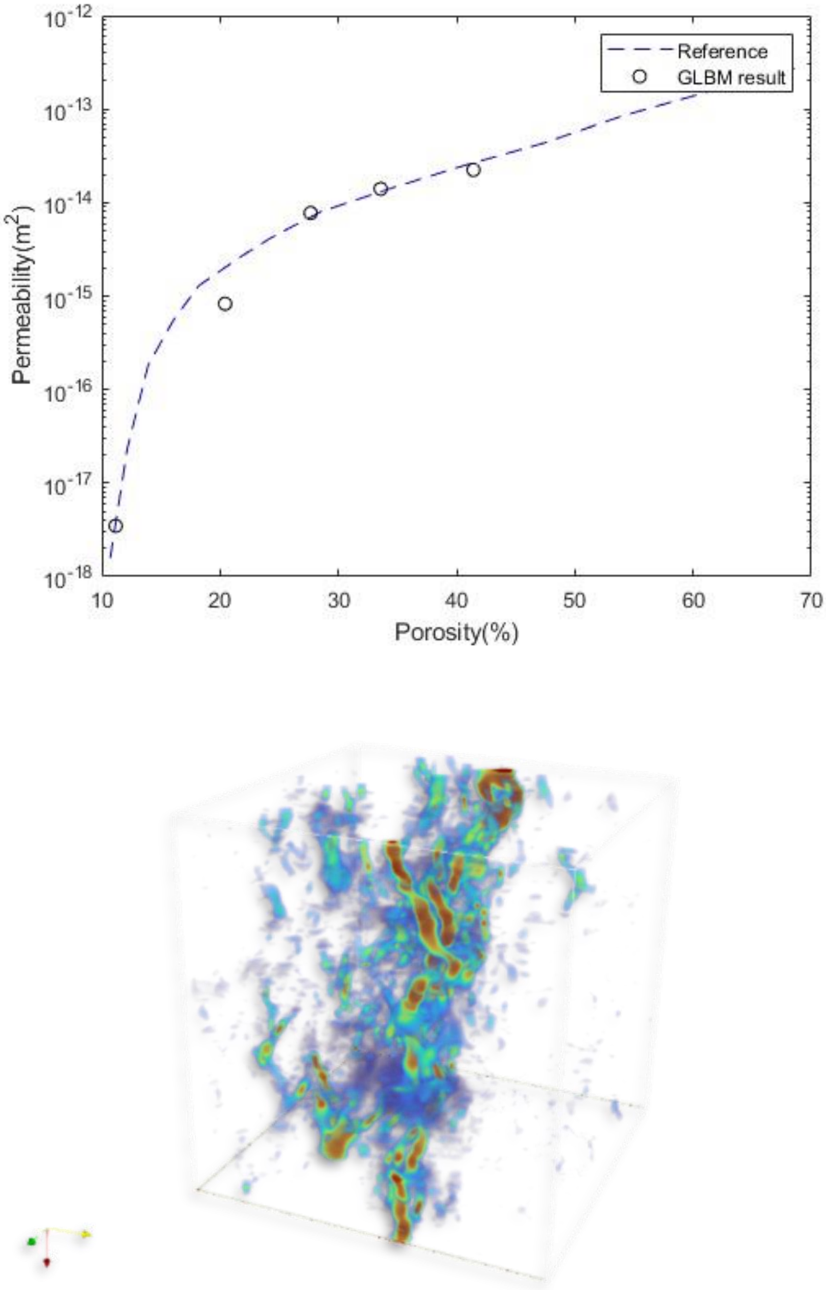

Figure 15. Simulated permeability to porosity graph
and the visualization of the simulation

3.3. Speedup and Convergence of the Simulation

Speedup of the program was 7.28 for 18 processors and showed the decrease of speedup ratio as number of processors increased. The efficiency of the parallelization is dependent on overhead of communication and the time for the calculation. Therefore, the decrease of speedup ratio can be explained with the size of domain used for the simulation. Due to the memory limit of the computer, domain was not large enough. The overhead of the communication is dominant for the efficiency of the parallelization as the small domain poses small amount of calculation. Also, as hybrid parallelization strategy was adopted, overhead for small problems had much larger effect on speedup. Therefore, it is expected that larger mesh density or large domain would result in greater speedup as effect of overhead would decrease.

Error graph showed exponential decay as depicted in Fig 16. The sample with water-to-cement ratio of 0.4 which has the simplest geometry and the sample with water-to-cement ratio of 0.7 which has the largest porosity showed the fast convergence compared to other samples. Every simulation has reached threshold of 10^{-6} with the error measurement of normalized L2 norm of energy as the test case for the cemented sandstone sample.

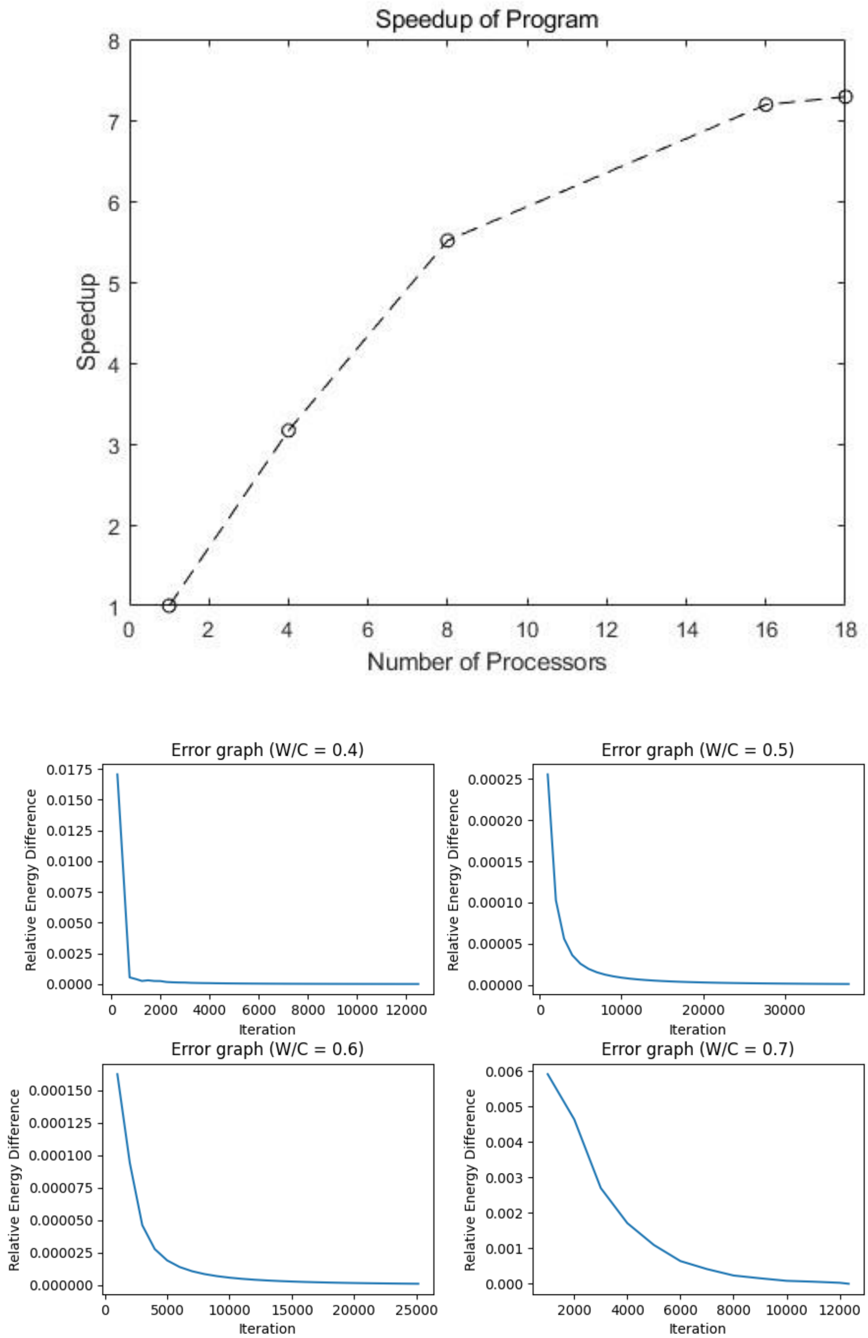

Figure 16. Speedup and convergence of the simulation

Chapter 4. Conclusion

The study has proposed the numerical method to analyze the permeability characteristics of the cementitious materials with percolated pore structure due to the limitations in the resolution of observation. The method has its strength in inclusion of capillary pore effect on the permeability of cementitious materials and its capability for the image-based permeability analysis which cannot be conducted by other numerical methods.

The results of the simulations recovered the tendency of the relationship between permeability and water-to-cement ratio. The results were accurate compared to the simulation results.

Also, the exceptional parallelization capability of the lattice Boltzmann method is utilized. Hybrid MPI-OpenMP parallelization strategy for the lattice Boltzmann method is proposed and the efficiency for small domain was tested. The case for the small domain showed good speedup. As the overhead for the communication due to the hybrid parallelization would decrease in larger domain, the efficiency of the parallelization would increase for the mesh with large element.

The limitation of the simulation can be written as follows. First, the real built environment could not be represented. Saturation of the pore structure and permeable media that represents the built environment can be achieved with the two-phase GLBM for water and air which would be the remedy for the limitation. Additionally, the effect of the capillary pores for the cementitious material is still in research. Therefore, the solid fraction values used in the research can be improved with more fundamental understanding about the capillary pore effect on permeability characteristics of the cementitious materials. At last, the method has memory problem when the sample size is large. This can be improved with coupling of the lattice Boltzmann method and finite element method. The coupling would be able to make simulation efficient and also would enable the method to simulate the permeability of the concrete.

Bibliography

[1] A. C1585-13, “Standard Test Method for Measurement of Rate of Absorption of Water by Hydraulic-Cement Concretes”. 22 Sep 2020.

[2] A. C666-97, "Standard Test Method for Resistance of Concrete to Rapid Freezing and Thawing". 16 Aug 2017.

[3] A. C1556, "Standard Test Method for Determining the Apparent Chloride Diffusion Coefficient of Cementitious Mixtures by Bulk Diffusion". 21 Nov 2022.

[4] A. Mouin and Z. Reza, "Finite-Volume Computations of Shale Tortuosity and Permeability From 3D Pore Networks Extracted From Scanning Electron Tomographic Images.," *Petrophysics,* vol. 60, p. 397–408, 2019.

[5] X. Li, Q. Xu and S. Chen, "An experimental and numerical study on water permeability of concrete," *Construction and Building Materials,* vol. 105, pp. 503-510, 2016.

[6] J. Pae, Y. Zhang, L. H. Poh and J. Moon, "Three-dimensional transport properties of mortar with a high water-to-cement ratio using X-ray computed tomography," *Construction and Building Materials,* vol. 281, 2021.

[7] T. Kruger, H. Kusumaatmaja, A. Kuzmin, O. Shardt, S. Goncalo and E. M. Viggen, The Lattice Boltzmann Method, Principles and Practice, Springer Cham, 2017.

[8] O. Dardis and J. McCloskey, "Lattice Boltzmann scheme with real numbered solid," *Physical Review E,* 1998.

[9] S. D. Walsh, H. Burwinkle and M. O. Saar, "A new partial-bounceback," *Computers & Geosciences,* vol. 35, no. 6, pp. 1186-1193, 2009.

[10] S. S, The Lattice Boltzmann Equation for Fluid Dynamics and Beyond, Oxford: Clarendon Press, 2001.

[11] Tracz and Tomasz, "Open porosity of cement pastes and their gas permeability.," *Bulletin of the Polish Academy of Sciences Technical Sciences,* 2016.

[12] M. Zalzale, "A 3D lattice Boltzmann effective media study: understanding the role of C-S-H and water saturation on the permeability of cement paste," *Modelling Simul. Mater. Sci. Eng.,* 2013.

[13] M. Zhang, "Pore-scale modelling of relative permeability of cementitious," *Cement and Concrete Research,* vol. 95, pp. 18-29, 2017.

[14] Z. M and M. P.J, "Lattice Boltzmann simulations of the permeability and capillary absorption of cement model microstructures," *Cement and*

Concrete Research, vol. 42, no. 12, pp. 1601-1610, 2012.

[15] P. Taylor, F. Bektas, E. Yurdakul and H. Ceylan, "Optimizing Cementitious Content in Concrete Mixtures for Required Performance.," 2012.

초록

전 세계적으로 구조물의 노후화로 인해 구조물 스마트 유지관리의 필요성이 증가하고 있다. 기존의 사회기반 시설들은 콘크리트로 시공되기 때문에 투수 계수 측정 또는 이온 확산 계수 측정 등 실험적 방법들을 활용하여 콘크리트 내구성 평가를 진행하고 있으나, 비파과적인 방법이나 다양한 환경을 고려한 수치해석 방법과 같은 스마트 구조물 유지 방법은 적용되지 못하고 있는 상황이다. 실험적 방법들은 실제 구조물에서 큰 샘플을 채취하여 시편을 파괴하면서 긴 시간동안 측정을 해야하는 단점을 가지고 있고, 기존의 수치해석적 방법들은 이미지의 해상도와 콘크리트와 같은 복잡한 공극 구조에 대한 해를 구하는 어려움 등의 한계를 가지고 있다.

본 연구에서는 이러한 한계를 극복하기 위한 수치해석적 방법인 격자 볼츠만 방법을 활용한 투수 계수 평가 방법을 제시하였다. 본 연구의 중점은 이미지의 해상도보다 작은 공극 구조를 고려한 효율적인 이미지 기반 수치 해석 방법의 개발에 있다. 이를 위하여 Hybrid MPI-OpenMP 병렬화를 활용한 회색 격자 볼츠만 방법이 제안하였다. 회색 격자 볼츠만 방법을 활용한 프로그램의 수렴성과 정확도를 연결된 공극을 갖는 모르타르 샘플을 통하여 확인하였다. 그리고 본 방법을 이미지 해상도 이하의 공극으로 인해 비연결 공극을 갖는 물 시멘트비가 서로 다른 Ordinary Portland Cement 샘플들에 대하여 적용하였다. 시뮬레이션은 빠른 속도를 보였고, 결과는 실험값의 경향성을 복원하고, 기존 시뮬레이션 연구들의 결과와 비교하여 정확했다. 개발된 방법은 사회기반 시설들의 스마트 유지관리에 활용될 수 있으며, 더 나아가 기존의 콘크리트의 투수 계수 평가를 위한 이미지 기반 시뮬레이션 방법들의 한계를 극복하는 방법 및 차후 연구를 통한 개선점이 제시되었다.